JOURNAL OF GEOPHYSICAL RESEARCH, VOL. 104, NO. D20, PAGES 24,547–24,555, OCTOBER 27, 1999

A comparison of cloud top heights computed from airborne lidar and MAS radiance data using CO_2 slicing

Richard A. Frey,[1] Bryan A. Baum,[2] W. Paul Menzel,[3] Steven A. Ackerman,[1] Christopher C. Moeller,[1] and James D. Spinhirne[4]

Abstract. Data from two instruments onboard the National Aeronautics and Space Administration (NASA) ER-2 high-altitude aircraft have been utilized in the largest validation study to date in assessing the accuracy of the CO_2-slicing cloud height algorithm. Infrared measurements of upwelling radiance from the MODIS (Moderate-Resolution Imaging Spectroradiometer) airborne simulator (MAS) were used to generate cloud top heights and then compared to those derived from the Cloud Lidar System (CLS), operating with dual polarization at 0.532 μm. The comparisons were performed for 10 flight days during the Subsonic Aircraft Contrail and Cloud Effects Special Study (SUCCESS) field experiment during April and May 1996 which included various single-layer and multilayer cloud conditions. Overall, the CO_2-slicing method retrieved cloud heights to within $\pm$500 m and to within $\pm$1500 m of the lidar heights in 32 and 64% of the cases, respectively. From a simulation of cloud height errors as a function of various error sources in the CO_2-slicing algorithm, it was concluded that the problem of multilayer clouds is secondary to that of proper specification of clear-sky radiances.

1. Introduction

Clouds have a large impact on the Earth's water and energy budgets. Their impact on the radiation budget can result in a heating or in a cooling of the planet, depending on the radiative properties of a cloud and its altitude [*Stephens and Webster*, 1981; *Stephens et al*., 1990]. Cloud vertical distributions, which vary considerably [*Stowe et al*., 1989; *Rossow et al*., 1989; *Wylie and Menzel*, 1989], determine diabatic heating profiles and hence affect the general circulation of the atmosphere. General circulation model (GCM) simulations demonstrate the impact of changes in cloud amount and vertical structure on atmospheric circulations [*Sinha and Shine*, 1995; *Stubenrauch et al*., 1997]. Therefore knowledge of cloud altitude and its variation in space and time is crucial to global climate change studies.

One important passive remote sensing method of obtaining the altitude of middle and upper level clouds, especially transmissive clouds, is the CO_2-slicing algorithm [*Smith et al*., 1974; *Chahine*, 1974; *Smith and Platt*, 1978; *Menzel et al*., 1983]. Previous investigators have implemented the algorithm using relatively low spatial-resolution input data such as the High-Resolution Interferometer Sounder (HIS), the High-Resolution Infrared Sounder (HIRS), and the Visible-Infrared Spin Scan Radiometer Atmospheric Sounder (VAS). *Wylie and Menzel* [1989] have shown that the method retrieves cloud heights with an overall accuracy of $\pm$5 kPa, while other studies have considered various associated sources of errors [*Smith and Platt*, 1978; *Wielicki and Coakley*, 1981; *Menzel et al*., 1992; *Baum and Wielicki*, 1994]. Other studies have compared CO_2-slicing cloud heights with those computed from lidar data [*Smith and Platt*, 1978; *Wylie and Menzel*, 1989; *Smith and Frey*, 1990] but with a somewhat limited number of samples and over a small geographical area.

This paper assesses the capabilities of the CO_2-slicing algorithm for inferring cloud top altitude using observations from the MODIS (Moderate-Resolution Imaging Spectroradiometer) airborne simulator (MAS) [*King et al*., 1996], a 50-m resolution spectrometer flown on high-altitude aircraft. Visible and infrared observations from the MAS are being used to develop MODIS at-launch algorithms. The retrieved cloud top altitudes are compared to simultaneous lidar observations [*Spinhirne and Hart*, 1990]. More than 4700 collocated observations are used to validate the CO_2-slicing cloud altitudes. Investigations were conducted to explain the distribution of cloud height differences and the most likely reason(s) for biases found between some lidar and CO_2-slicing cloud heights.

2. Data

During the Subsonic Aircraft Contrail and Cloud Effects Special Study (SUCCESS) field campaign [*Toon and Miake-Lye*, 1998], measurements of both clear and cloudy scenes were taken by several instruments onboard the NASA ER-2, a high-altitude (20 km) research aircraft. Two of those instruments were the MAS, a 50-channel spectrometer operating in the visible, near-infrared, and infrared wavelengths, and the Cloud Lidar System (CLS) [*Spinhirne and Hart*, 1990], a dual-polarization lidar operating at 0.532 μm. Both instruments are designed to provide detailed information concerning cloud characteristics such as altitude and structure. The CLS field of view (FOV) is nominally 20 m at the surface for an aircraft altitude of 20 km, but the raw data are usually averaged over some period of time (between 3 and 13 s during the SUCCESS mission) according to the quality of the lidar signal. An aver-

[1]Space Science and Engineering Center, University of Wisconsin, Madison.
[2]Atmospheric Sciences Division, NASA Langley Research Center, Hampton, Virginia.
[3]Satellite Applications Laboratory, NOAA NESDIS, Madison, Wisconsin.
[4]NASA Goddard Space Flight Center, Greenbelt, Maryland.

Paper number 1999JD900796.
0148-0227/99/1999JD900796$09.00

aging time of 5 s implies a ground resolution of 20 × 1000 m since the ER-2 travels at a speed of 200 m/s. The CLS views only at the nadir position. The MAS instrument has a FOV of ~50 m at the surface and scans through ~90° centered on nadir (scan angle of zero degrees).

The MAS cloud mask [*Ackerman et al*., 1998], developed at the Cooperative Institute for Meteorological Satellite Studies, was used to screen the data for clear-sky FOVs.

Daily 0000 and 1200 UT temperature and moisture profiles were obtained from National Weather Service (NWS) radiosonde data. These profiles (typically within 5 hours and 150 km of the lidar and MAS observations) were used as input to the CO_2-slicing algorithm, but single profiles were used for multiple cloud height calculations, because of the relatively coarse spatial and temporal resolution of NWS radiosonde launches. A total of 15 separate profiles were used in the study.

Data were processed from 10 separate days during the months of April and May 1996 in locations ranging from the states of Texas to Nebraska in the central United States and westward as far as Colorado in the Rocky Mountains. Three other days (April 20, 27, and May 8) with collocated MAS and CLS data were not included in the comparisons because of obvious biases between clear-sky brightness temperatures measured by the MAS and nearby available NWS temperature profile data.

Table 1 shows the distribution of cloud height retrievals by date and various cloud conditions. The differences between the numbers of cloud height retrievals and the total collocations are due to the presence of clear skies, clouds detected by the lidar but not the MAS cloud mask and vice versa, or very small cloud-forcing values which are smaller than the instrument sensitivity. Note that cloud observations may fall into more than one category and that many multilayer clouds are also optically thin. When lidar data indicate a single-layer thick cloud, the assumption is made that no clouds are present beneath.

3. Technique

Cloud heights inferred from MAS and CLS data are compared in this study. The CLS lidar cloud height results are compared to those obtained from the CO_2-slicing algorithm using MAS data. The CLS data provide cloud top and base altitudes for a maximum of five cloud layers. The data are provided by *Spinhirne et al*. [1997] and are available via the Internet. Most details of the CO_2-slicing algorithm are not presented here, as we closely follow the method of *Wylie and Menzel* [1989], excepting spectral band selection due to different instrumentation and the use of calculated clear-sky radiances instead of observed. There are three longwave IR channel pairs found on the MAS instrument which may be used for CO_2-slicing cloud height assignment. They are the 11.0 and 13.3, 13.3 and 13.8, and the 13.8 and 14.3 μm pairs. Wylie and Menzel do not use the 11.0- and 13.3-μm channel combination. It is used here only when a determination was made that the cloud being viewed by the MAS was most likely an ice cloud. The 8.5- and 11.0-μm brightness temperature differences were used to make this distinction because of increasing absorption by ice across this spectral interval [*Strabala et al*., 1994]. Cloud scenes with 11.0-μm brightness temperatures at least 2K less than the corresponding 8.5-μm brightness temperatures are labeled as ice. An assumption of the CO_2-slicing method is that the cloud emissivities of the channel pairs are the same [*Smith et al*., 1974]. Water cloud emissivities between the 11.0- and the 13.3-μm channels can differ to an extent that the CO_2-slicing result would be in doubt.

Since the CLS is nadir viewing, only those CO_2-slicing cloud heights from near the center of the MAS data swaths are used in the comparison. Averaged radiance data from groups of 100 FOVs (10 × 10 boxes) centered as near as possible to nadir are used. The average is taken to improve the signal-to-noise ratio of the MAS radiances. Since 10 scan lines of MAS data are gathered in about 1.5 s, there are many instances where more than one MAS 10 × 10 FOV group falls within the averaging period of the CLS data. In these cases the CO_2-slicing cloud heights are averaged and then compared to the lidar value.

The temperature and moisture profiles are used as input to a forward radiative transfer model for calculation of clear-sky radiances and for computations of spectral cloud forcing in the CO_2-slicing algorithm. Generally, the closest NWS radiosonde data to the aircraft flight track are used; however, obvious profile errors necessitate the use of alternative sites (but still nearby) in a few cases. Most of the aircraft data were taken from about 1700 to 2100 UT, so the 0000 UT profiles corresponded more closely than the 1200 UT profiles to atmospheric conditions during the flights. Time interpolation of the profiles was not attempted. Differences between ER-2 flights and radiosonde times would have significant effects only on surface and near-surface temperatures in the fair weather situations in which these flights took place. The CO_2-slicing algorithm is relatively immune to surface temperature errors [*Menzel et al*., 1992] since upwelling radiation from the surface contributes little to the total measured radiances of the CO_2

Table 1. Distribution of Collocated CLS and MAS Data by Date and Cloud Condition

Date	Number of Collocated Regions	Cloud Retrievals	Single-Layer Clouds	Optically Thin Clouds	Boundary Layer (BL) Clouds Only	Single-Layer, Thin, Non-BL Clouds
April 13	941	74	7	52	0	7
April 15	1101	5	5	5	5	0
April 16	1414	495	211	453	0	175
April 21	1220	1123	227	642	8	33
April 23	809	418	155	180	0	66
April 26	401	7	6	7	0	6
May 2	901	732	76	235	6	6
May 3	2442	286	248	138	248	0
May 4	2652	517	468	170	468	0
May 7	1180	1091	209	318	187	35
Totals	13061	4748	1612	2200	922	328

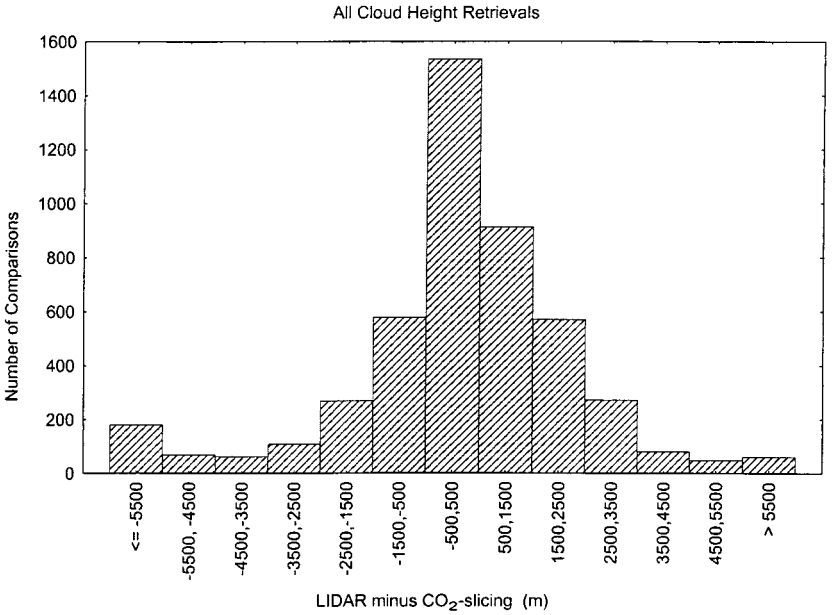

Figure 1. Histogram of differences for all comparisons between Cloud Lidar System (CLS) and CO_2-slicing cloud heights in meters.

absorption channels, which are most sensitive to the middle and upper atmosphere.

The MAS cloud mask is queried before the CO_2-slicing algorithm is performed. If more than 10 FOVs are found to be cloudy, then a cloud height is computed for that 10×10 FOV area.

4. Results and Discussion

As a result of the differing times and resolutions of the CLS and MAS cloud products, comparisons of cloud top heights from the two data sets are somewhat problematic. The MAS retrievals in the across-track direction, based on 10×10 groups of FOVs, extend ~250 m on either side of the nadir position [*King et al*., 1996] while that of the CLS is only about 10 m [*Spinhirne and Hart*, 1990]. When observing broken cloud fields, fractional cloud coverage can be very different between the two scenes. Even when cloud fields cover the entire area of both instruments' FOVs, the optical depth may change from one part of the field to another, possibly leading to substantial differences between retrieved cloud heights. Of course, there is also the fact that the lidar is capable of finding the very top of the uppermost cloud layer, while the IR MAS radiances emanate mostly from some level beneath the top of the cloud, depending on the emissive characteristics of the cloud. With these caveats in mind, we will show that the CO_2-slicing algorithm may successfully be used to characterize cloud heights from IR data collected during the SUCCESS mission.

Figure 1 shows a histogram of all differences between cloud top heights as retrieved from CLS data and from the CO_2-slicing algorithm. The difference values are calculated as the CLS height of the top of the uppermost layer of cloud (as reported in the CLS data) minus the collocated CO_2-slicing value. We consider the lidar values to be "truth." The distribution of differences is approximately Gaussian with more CO_2-slicing results falling into the ± 500 m difference category than any other. At an altitude of 10 km in a U.S. standard atmosphere, 500 m corresponds to ~2 kPa, while 2000 m is roughly equivalent to 8 kPa. This is an encouraging result, because this figure represents all retrievals, including multilevel cloud cases. These values match well with the error analysis performed by *Wylie and Menzel* [1989], where they showed that CO_2-slicing cloud heights from VAS data are accurate to within 5 kPa.

Figure 2 is a bivariate histogram showing a comparison of cloud top heights from both methods. Perfect agreement be-

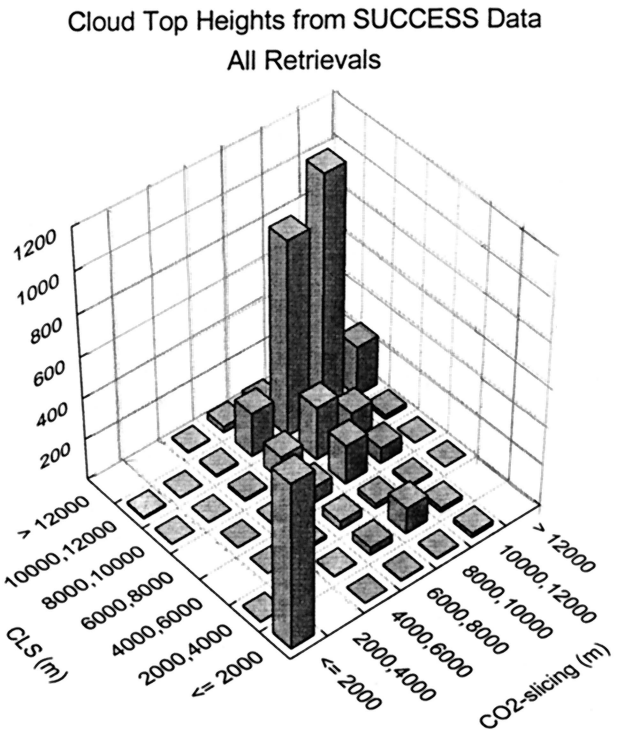

Figure 2. Bivariate histogram showing a comparison of cloud top heights from MODIS airborne simulator (MAS) CO_2-slicing and CLS lidar.

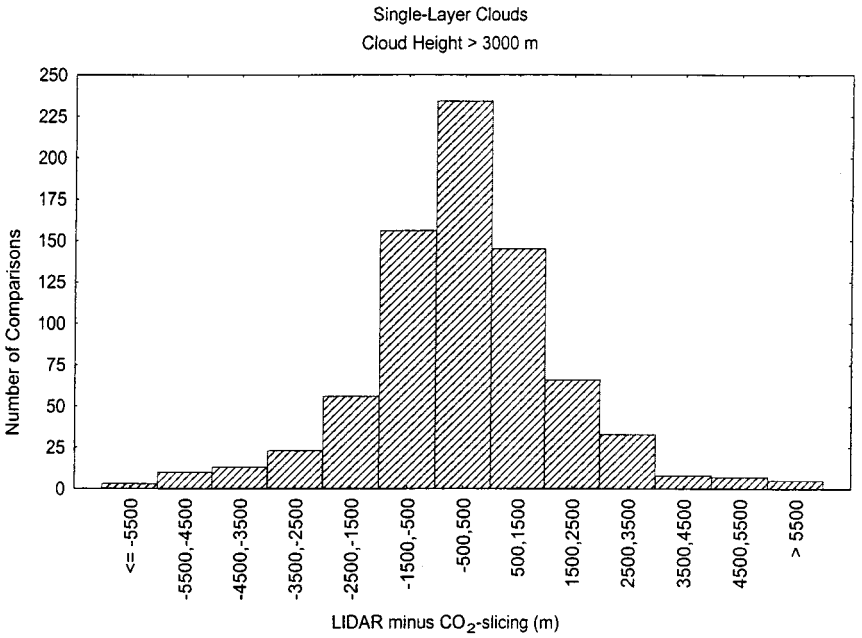

Figure 3. Histogram of differences between CLS lidar and CO_2-slicing cloud heights in meters. Clouds are single-layer with tops >3000 m.

tween the two would place a diagonal row of columns from top to bottom in the diagram. The values in the two data sets agree to within 2 km in the large majority of cases. As expected, one sees more scatter at higher cloud altitudes because of the higher occurrence of semitransparent cirrus clouds and multilayer clouds. Since the SUCCESS experiment focused on jet contrails and cirrus clouds, there are few midlevel cloud cases indicated in the figure. The "pole" seen at the bottom of the figure represents boundary layer cloud retrievals.

With airborne lidar data, one can specify very accurately features of the observed cloud fields [*Spinhirne and Hart*, 1990; *Spinhirne et al.*, 1982]. The geometric and relative optical thicknesses, height, and stratification of clouds may be easily and accurately ascertained. In the following sections we will compare CO_2-slicing cloud heights with those indicated by lidar as a function of cloud type.

4.1. Single-Layer Clouds With Indications of Optical Depth

Figure 3 shows a histogram of cloud height differences between the two methods for all single-layer cloud comparisons

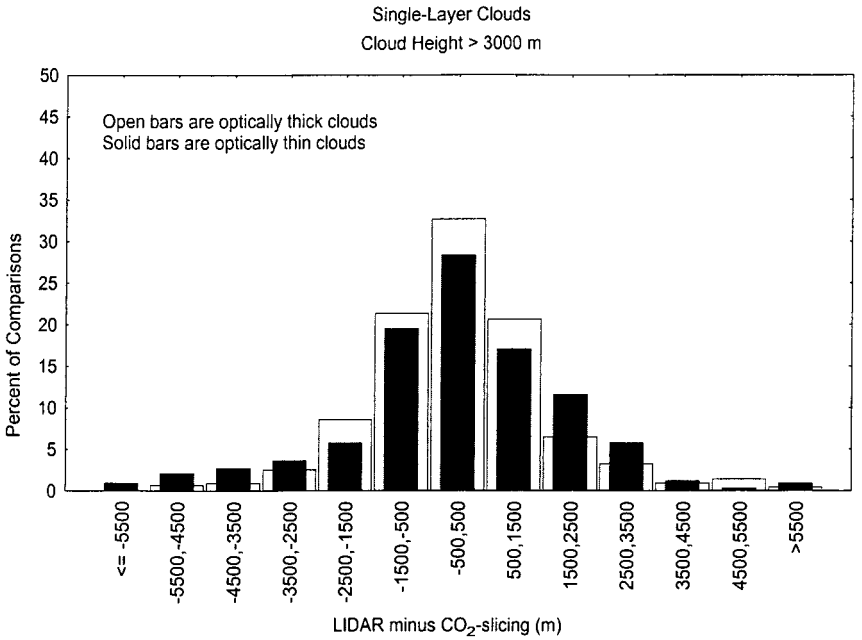

Figure 4. Histogram of differences between CLS lidar and CO_2-slicing cloud heights in meters. Clouds are single-layer with tops >3000 m. Open bars represent optically thick clouds, while solid bars show optically thin cloud retrievals.

where cloud top heights were >3000 m. Again, the shape of the distribution is roughly Gaussian. This figure does not include boundary layer clouds, which are usually assigned a height by simply comparing observed 11 μm brightness temperatures to the appropriate temperature profile. The assumption is made that these clouds radiate as blackbodies. This procedure is necessary in the case of scenes containing only low clouds because the difference between clear-sky and observed radiance values often falls within the instrument noise limits, and the CO_2-slicing method cannot be used. These limits are 0.25, 0.75, 2.00, and 2.50 w/m^2/steradian/μm for the 11.0-μm, 13.2-μm, 14.0-μm, and 14.2-μm bands, respectively.

Figure 4 shows results for single-layer cloud scenes but also distinguishes between optically thin and optically thick clouds. When no clouds are present in the FOV of the CLS, the pulse of light from the instrument easily reaches the ground with a portion reflected back to the receiver on the ER-2. However, if clouds are present and are of sufficient optical depth, the ground signal is significantly weakened or attenuated completely. The ground signal is completely attenuated when the total columnar aerosol and cloud optical depth exceeds 3.0 (W. D. Hart, personal communication, 1999). This information is used as an indicator of optical thickness. Thick clouds are defined as those for which no surface signal was present in the CLS data. Conversely, optically thin clouds are those cases where a cloud and a surface signal are both present in the lidar data and the CO_2-slicing method is able to retrieve a cloud height. Since the lidar is sensitive to extremely thin clouds, sometimes the IR cloud signal (clear - cloudy radiance) falls within the MAS instrument noise limits and no retrieval is possible. Notice that the class of maximum frequency is $\pm$500 m and that a large majority of the results fall between $\pm$1500 m for both thin and thick clouds. The shapes of the histograms differ, however, with thick cloud errors showing a narrower and more normal distribution. The thin cloud results also contain a slight bias toward positive differences.

These outcomes agree well with simulations. Following the method of *Baum and Wielicki* [1994], the effects of several error sources on CO_2-slicing cloud heights were investigated, including instrument noise and errors in the temperature profile used as input to radiative transfer calculations. Sets of 500 samples were constructed for 30-kPa cirrus clouds at several effective cloud amounts, $N\varepsilon$ (the product of cloud fraction N and cloud emmisivity ε). Instrument noise was assumed to be Gaussian with a zero mean and standard deviations equal to the noise-equivalent radiances for the MAS channels [*King et al*., 1996]. Instrument noise errors were added to the radiances calculated from a radiative transfer model using a climatological midlatitude temperature and moisture profile. Errors in the temperature profile were modeled as Gaussian about the given temperature at each pressure level with a standard deviation of 2°.

The four histograms in Figures 5a–5d show simulations of cloud height errors ("truth" minus realization) due to instrument noise alone and temperature profile errors and instrument noise combined for a cirrus cloud at 30 kPa and $N\varepsilon$ = 0.3, 0.4, 0.5, and 0.6. In the thicker cloud cases (Figures 5c and 5d), both histograms show a Gaussian distribution with most cloud heights within 500 m of "truth." In the case of thinner clouds (Figures 5a and 5b), deviations due to combined instrument noise and profile errors show a much wider distribution, primarily because the cloud signals (clear minus cloudy radiances) are much smaller. This agrees with the results shown in Figure 4. Given these error sources, one may expect a distribution of retrieved cloud heights both above and below the truth, but biases will be absent.

There were situations where errors resulted in biased cloud heights, however. As noted above, cloud height retrievals from several days during SUCCESS were discarded because of biases between MAS brightness temperatures and radiosonde measurements. For example, on April 27, MAS data were collected over northern Oklahoma, but the Norman, Oklahoma, radiosonde was unavailable. The Topeka, Kansas, profile was used instead. By comparing temperature profile data from the CART (cloud and radiation test bed) site in Lamont, Oklahoma, to the Topeka data, it was found that the Topeka profile was quite a bit colder, ranging from about 10° near the surface to about 2° in the upper troposphere. Figure 6 shows the actual cloud height deviations from "truth" (lidar cloud heights) when such a temperature bias exists, while Figure 7 shows modeled errors. Simulations are shown for the combined effects of instrument noise, a cold bias in the temperature profile of 2K (at all levels except the surface), and a surface temperature cold bias of 5K. It is interesting to note that at low effective cloud amounts (Figures 7a and 7b) the errors due to instrument noise dominate errors due to biases in the temperature profile, as seen by the spread of simulated cloud height errors. As the effective cloud amount increases from 0.5 (Figure 7c) to 0.6 (Figure 7d), the bias in retrieved cloud heights due to the temperature profile errors becomes more pronounced. However, there is still some spread in the results due to instrument noise. In future MODIS processing, there will be an attempt to correct for biases between temperature profiles and radiometric measurements by comparing observed clear-sky brightness temperatures (collected during the cloud-masking process) with calculated values within a reasonable area and time. *Frey et al*. [1996] used this method with good success in processing global HIRS 2 data. If most biases can be removed, one may aggregate cloud height retrievals over space and time with added confidence.

4.2. Multilayer Clouds

The CLS instrument makes it possible to validate CO_2-slicing cloud top heights for multilayer cloud scenes. Figure 8 shows the distribution of differences between the lidar and the CO_2-slicing results for the entire validation data set when there are two (but only two) cloud layers separated by at least 6000 m. The $\pm$500-m difference class contains the most occurrences, and the shape of the histogram is approximately Gaussian, but there is a "tail" of very low cloud heights. This tail represents scenes where the top layer of cloud is very thin and most of the emission measured by the MAS is coming from the lower layer of cloud. Again, simulations help explain the shape of the observed distribution of cloud height errors. The top two histograms (Figures 9a and 9b) show modeled distributions of errors due to instrument noise and the presence of low clouds at 80 kPa, along with a 30-kPa cirrus cloud with $N\varepsilon$ = 0.3 and 0.6. Since climatologies suggest that about half of cloud observations are of multilayered clouds [*Hahn et al*., 1982, 1984], $N\varepsilon$ for the low clouds is set to zero for half of the realizations, but in the other half, $N\varepsilon$ is allowed to vary between zero and 100%. The third and fourth histograms (Figures 9c and 9d) show the same simulations except that random temperature profile noise has also been included. As the upper cloud gets optically thicker, the distribution of errors narrows and becomes approximately Gaussian with little bias, unlike the case

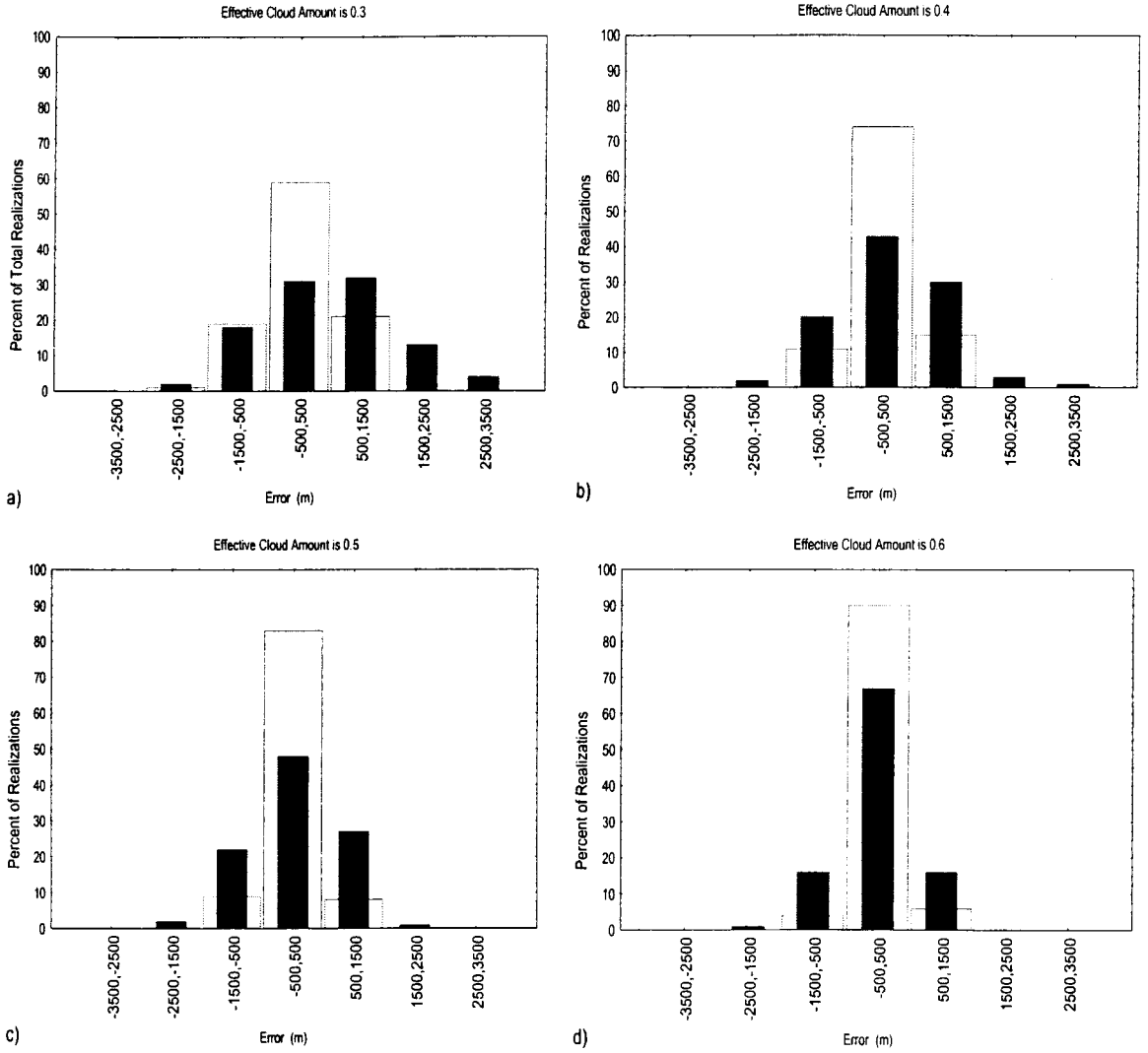

Figure 5. Simulated cloud height errors for a cirrus cloud at 30 kPa due to instrument noise (open bars) and atmospheric profile noise plus instrument noise (solid bars). Figures 5a–5d are for effective cloud amounts ranging from 0.3 to 0.6.

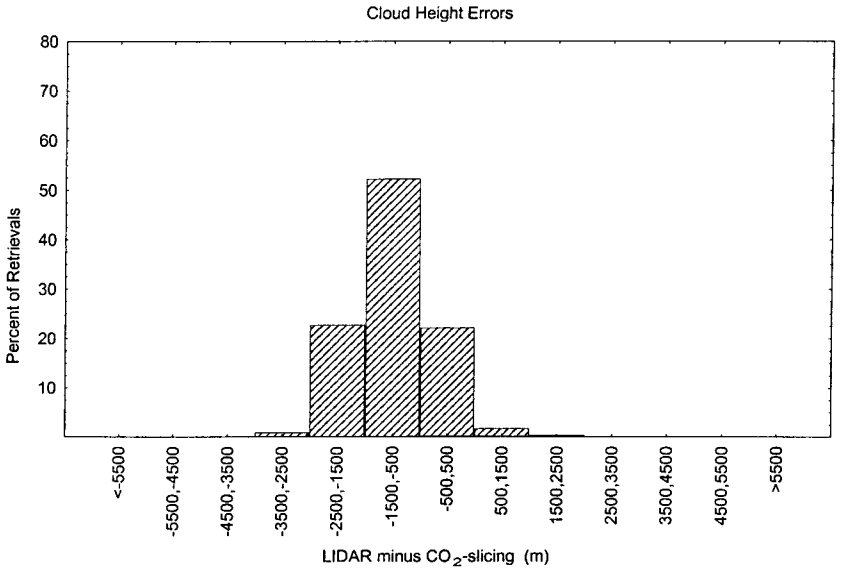

Figure 6. Distribution of cloud height errors on April 27, 1996.

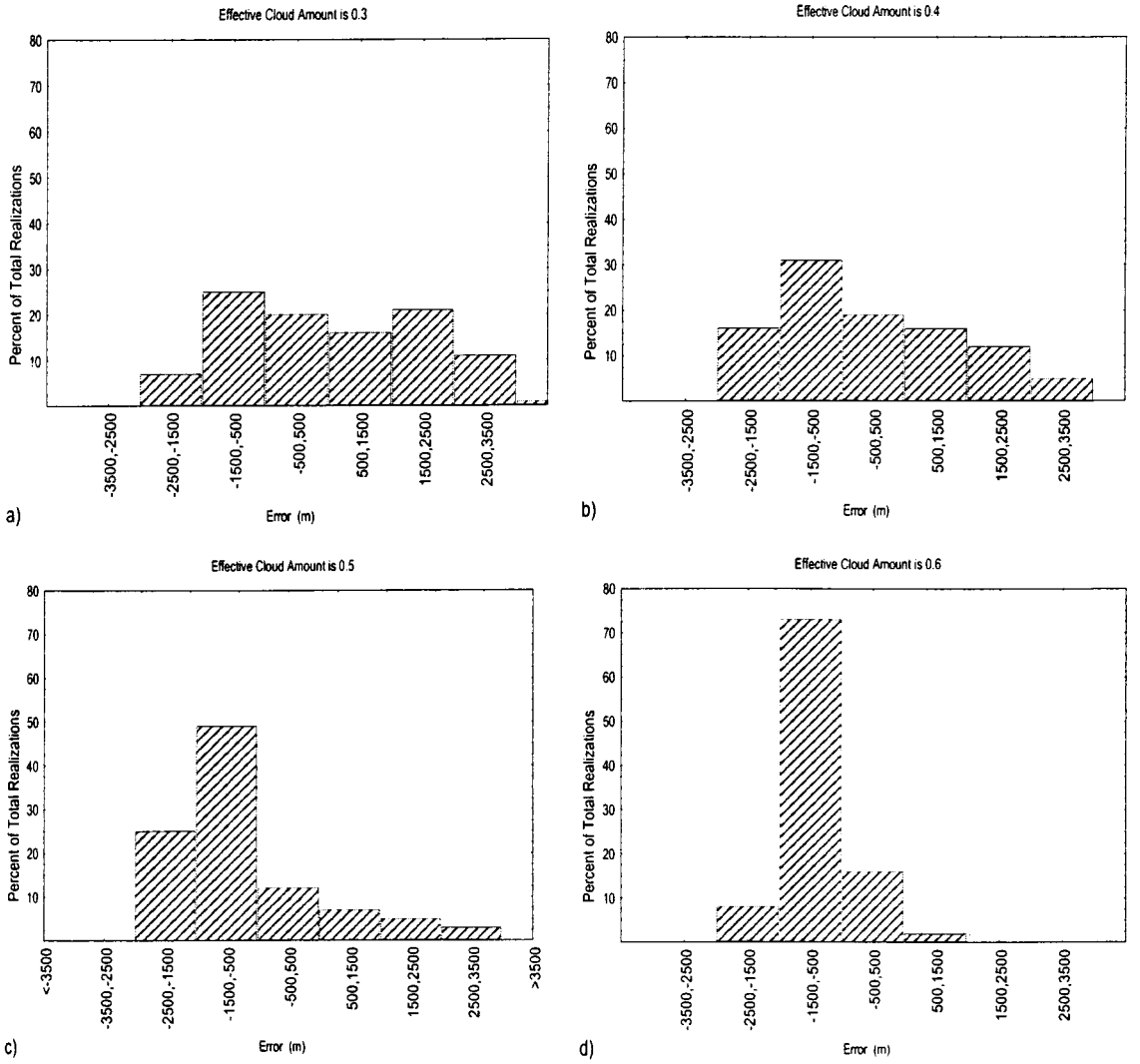

Figure 7. Distribution of simulated cloud height errors when a cold bias exists in the clear-sky temperature profile. Errors were derived using instrument noise plus a 2K cold bias in the temperature profile and a 5K cold bias in the surface temperature. Figures 7a–7d are for effective cloud amounts of 0.3–0.6, respectively.

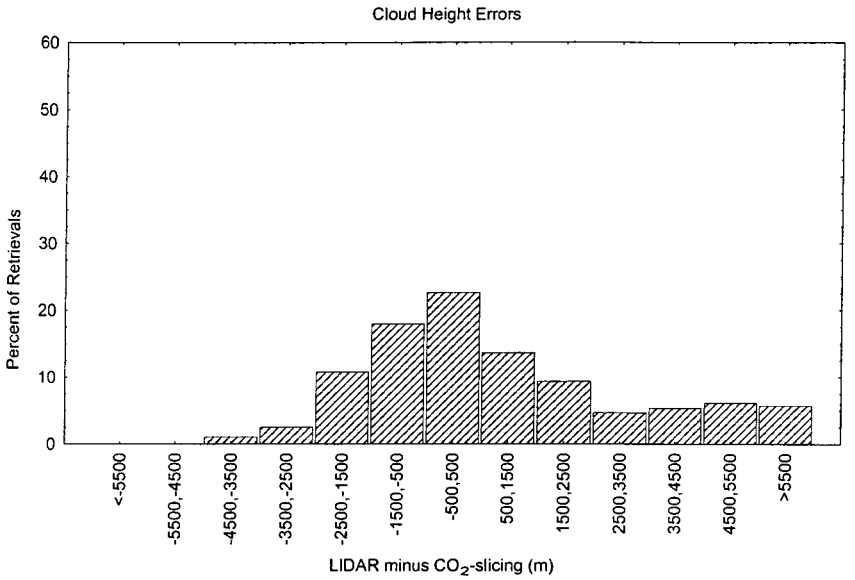

Figure 8. Distribution of cloud height errors when two layers of cloud are present. The two layers are separated by at least 6000 m.

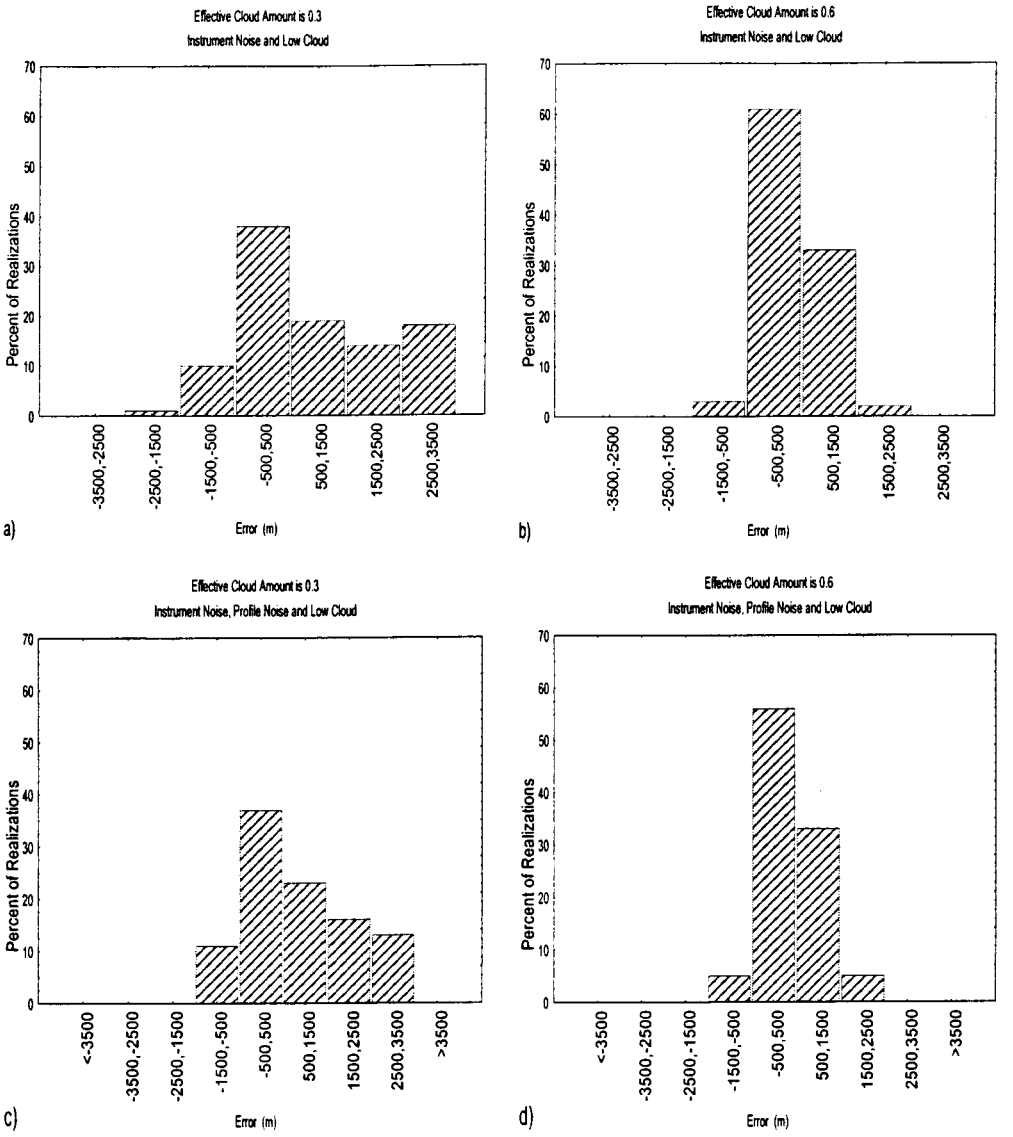

Figure 9. Distribution of simulated cloud height errors when two cloud layers are present. Top layer of cloud is at 30 kPa, while lower layer is at 80 kPa. Figures 9a and 9b are for instrument noise and low cloud, where the effective cloud amounts are 0.3 and 0.6, respectively. Figures 9c and 9d are the same, except atmospheric profile noise has been added.

of temperature profile bias shown in Figure 7. Even in the case of a very optically thin upper cloud (Figure 9a), almost 40% of realizations fall in the ±500-m class. The actual cloud height errors (Figure 8) have a distribution similar to the top, left histogram, implying that many of the actual SUCCESS two-layer clouds came from scenes where the cirrus layer was very optically thin. Nevertheless, the present algorithm appears to be sufficient for accurate determination of cloud top heights in many cases of two-layer clouds.

5. Conclusions

More than 4700 cloud top heights measured from CLS data and computed from MAS IR radiance data (using the CO_2-slicing method) during the SUCCESS field experiment were compared. This exercise was undertaken to evaluate the CO_2-slicing method much as it will be implemented in the processing of the future MODIS data. In the course of the study we have assembled the largest validation data set to date between CO_2-slicing cloud heights and lidar information, which we use as "truth."

Overall, the algorithm retrieved cloud heights to within ±500 m in 32% of cases and to within ±1500 m in 64% of the cases in the 10 days of SUCCESS cloud scenes studied. This is an encouraging result when one considers that 66% of all comparisons came from multilayer cloud situations. One factor to be noted about the SUCCESS data, which is both a benefit and a liability, is that most scenes contained only cirrus and/or underlying boundary layer clouds. This is a benefit in that cirrus clouds pose the most difficulty when assigning cloud height and therefore require more study, but a liability because very few midlevel clouds are included in the validation. Even in the cases of optically thin clouds (of which more than 72% were multilayer), 30 and 63% of retrieved cloud top heights were within ±500 and ±1500 m, respectively, of the lidar values.

From a simulation of cloud height errors as a function of various error sources in the CO_2-slicing algorithm, we concluded that observed temperature biases between radiosonde and radiometric data have a very negative influence on the results. Although more comparisons are required from diverse locations and measurement systems to increase confidence, it appears that the problem of multilayer clouds is secondary to that of proper specification of clear-sky radiances. Certainly, lower clouds beneath very optically thin clouds (effective cloud amount ≤ 0.3) lead to cloud height biases, but the overall effect is smaller than from the use of biased clear-sky radiances. For thicker but still transmissive clouds (effective cloud amount = 0.6), the clear-sky temperature bias effect clearly dominates that due to lower clouds. More work on the proper specification of clear-sky radiances for the purpose of cloud radiative studies is indicated.

Acknowledgments. This research was supported by NASA under grant NAS5-31367. The authors would also like to express gratitude to Kathy Strabala and Liam Gumley for their helpful suggestions.

References

Ackerman, S. A., K. I. Strabala, W. P. Menzel, R. A. Frey, C. C. Moeller, and L. E. Gumley, Discriminating clear-sky from clouds with MODIS, *J. Geophys. Res*., *32*,141–32,157, 1998.

Baum, B. A., and B. A. Wielicki, Cirrus cloud retrieval using infrared sounding data: Multilevel cloud errors, *J. Appl. Meteorol*., *33*, 107–117, 1994.

Chahine, M. T., Remote sounding of cloudy atmospheres, 1, The single cloud layer, *J. Atmos. Sci*., *31*, 233–243, 1974.

Frey, R. A., S. A. Ackerman, and B. J. Soden, Climate parameters from satellite measurements, 1, Collocated AVHRR and HIRS/2 observations of spectral greenhouse parameter, *J. Clim*., *9*, 327–344, 1996.

Hahn, C. J., S. G. Warren, J. London, R. M. Chervin, and R. Jenne, Atlas of simultaneous occurrence of different cloud types over the ocean, *NCAR Tech. Note*, *TN-201+STR*, 212 pp., Natl. Cent. for Atmos. Res., Boulder, Colo., 1982.

Hahn, C. J., S. G. Warren, J. London, R. M. Chervin, and R. Jenne, Atlas of simultaneous occurrence of different cloud types over land, *NCAR Tech. Note*, *TN-241+STR*, 209 pp., Natl. Cent. for Atmos. Res., Boulder, Colo., 1984.

King, M. D., et al., Airborne scanning spectrometer for remote sensing of cloud, aerosol, water vapor and surface properties, *J. Atmos. Oceanic Technol*., *13*, 777–794, 1996.

Menzel, W. P., W. L. Smith, and T. R. Stewart, Improved cloud motion wind vector and altitude assignment using VAS, *J. Appl. Meteorol*., *22*, 377–384, 1983.

Menzel, W. P., D. P. Wylie, and K. I. Strabala, Seasonal and diurnal changes in cirrus clouds as seen in four years of observations with the VAS, *J. Appl. Meteorol*., *31*, 370–385, 1992.

Rossow, W. B., L. C. Gardner, and A. A. Lacis, Global seasonal cloud variations from satellite radiance measurements, 1, Sensitivity of analysis, *J. Clim*., *2*, 419–458, 1989.

Sinha, A., and K. P. Shine, Simulated sensitivity of the Earth's radiation budget to changes in cloud properties, *Q. J. R. Meteorol. Soc*., *121*, 797–819, 1995.

Smith, W. L., and R. A. Frey, On cloud altitude determinations from high resolution interferometer sounder (HIS) observations, *J. Appl. Meteorol*., *29*, 658–662, 1990.

Smith, W. L., and C. M. R. Platt, Comparison of satellite-deduced cloud heights with indications from radiosonde and ground-based laser measurements, *J. Appl. Meteorol*., *17*, 1796–1802, 1978.

Smith, W. L., H. M. Woolf, P. G. Abel, C. M. Hayden, M. Chalfant, and N. Grody, Nimbus 5 sounder data processing system, 1, Measurement characteristics and data reduction procedures, *NOAA Tech. Memo*., *NESS 57*, 99 pp., Natl. Oceanic and Atmos. Admin., Washington, D. C., 1974.

Spinhirne, J. D., and W. D. Hart, Cirrus structure and radiative parameters from airborne lidar and spectral radiometer observations, *Mon. Weather Rev*., *118*, 2329–2343, 1990.

Spinhirne, J. D., M. Z. Hansen, and L. O. Caudill, Cloud top remote sensing by airborne lidar, *Appl. Opt*., *21*, 1564–1571, 1982.

Spinhirne, J. D., W. D. Hart, and D. Hlavka, Cloud Lidar System Onsite Quicklook Database, http://virl.gsfc.nasa.gov/~success/success.html., 1997.

Stephens, G. L., and P. J. Webster, Clouds and climate: Sensitivity of simple systems, *J. Atmos. Sci*., *38*, 235–247, 1981.

Stephens, G. L., S. C. Tsay, J. P. W. Stackhouse, and P. Flatau, The relevance of the microphysical and radiative properties of cirrus clouds to climate and climatic feedback. *J. Atmos. Sci*., *47*, 1742–1753, 1990.

Stowe, L. L., H. Y. M. Yeh, T. F. Eck, C. G. Wellemeyer, H. L. Kyle, and the Nimbus-7 Cloud Data Processing Team, Nimbus-7 global cloud climatology, II, first year results, *J. Clim*., *2*, 671–709, 1989.

Strabala, K. I., S. A. Ackerman, and W. P. Menzel, Cloud properties inferred from 8-12-μm data, *J. Appl. Meteorol*., *33*, 212–229, 1994.

Stubenrauch, C. J., A. D. Del Genio, and W. B. Rossow, Implementation of subgrid cloud vertical structure inside a global circulation model and its effect on the radiation budget, *J. Clim*., *10*, 273–287, 1997.

Toon, O. B., and R. C. Kiake-Lye, Subsonic aircraft: Contrail and cloud effects special study, *Geophys. Res. Lett*., *25*, 1109–1112, 1998.

Wielicki, B. A., and J. A. Coakley Jr., Cloud retrieval using infrared sounder data: Error analysis, *J. Appl. Meteorol*., *20*, 157–169, 1981.

Wylie, D. P., and W. P. Menzel, Two years of cloud cover statistics using VAS, *J. Clim. Appl. Meteorol*., *2*, 380–392, 1989.

S. A. Ackerman, R. Frey, and C. C. Moeller, 1225 W. Dayton St., Room 219, Space Science and Engineering Center, University of Wisconsin-Madison, Madison, WI 53706. (richard.frey@ssec.wisc.edu)

B. A. Baum, Atmospheric Sciences Division, NASA Langley Research Center, Hampton, VA 23665.

W. P. Menzel, Satellite Applications Laboratory, NOAA/NESDIS, Madison, WI 53706.

J. D. Spinhirne, NASA Goddard Space Flight Center, Greenbelt, MD 20771.

(Received January 21, 1999; revised June 3, 1999;
accepted July 13, 1999.)